Supporting Information

Operando Spectroscopy Investigations of the Redox Reactions in Heme and Heme-Proteins

Subhankar Mandal[1], Dipen Biswakarma[1], Aninda J. Bhattacharyya[1,2*]

[1]Solid State and Structural Chemistry Unit, Indian Institute of Science, Bengaluru: 560012, Karnataka, INDIA

[2]Interdisciplenary Center for Energy Research, Indian Institute of Science, Bengaluru: 560012, Karnataka, INDIA

*Aninda J. Bhattacharyya: anindajb@iisc.ac.in

Laviron Model:

Laviron model is used for heterogeneous rate constant and transfer coefficient for the surface adsorbed redox process. The bellow formalism is used for kinetic parameter:

$$E_p = E^0 + \frac{RT}{\alpha nF}\{\ln\left(\frac{RTKs}{\alpha nF}\right) - ln\,v\}$$

Where E_p is the peak potential of redox process, E_0 is the formal potential of the system, R is universal gas constant (8.314 J $K^{-1}mol^{-1}$), T is the absolute temperature (298 K), α is electron transfer coefficient of the electrode process, n is the number of electron participation in redox process, F is the Faraday constant (96485 C mol^{-1}), K_s is the heterogeneous electron transfer rate constant.

Calculation of % of reduced or oxidized Species:

Operando UV-vis spectroscopy is employed to calculate the % of reduced or oxidized species during redox process and the formal potential calculation. The following formalism is used to calculate the formal potential as well as number of electrons in the redox process.

$$\frac{[reduced\ form]}{[oxidzed\ form]} = \frac{A_0 - A_E}{A_E - A_R} \text{ ---------- [1]}$$

A_R is absorbance of proteins in fully reduced state, A_O is absorbance after complete oxidation, and A_E is the absorbance at different depth of potential. At the initial state of experiment, we assume all the species are in oxidized state. A_R is set as zero for the absorbance before the experiment. The above equation is:

$$\frac{[reduced\ form]}{[oxidzed\ form]} = \frac{A_0 - A_E}{A_E} = \frac{\Delta A}{A_E} \text{ ---------- [2]}$$

To formalized with Nernst equation with the above equation

$$E_{applied} = E^{0'} - \frac{0.059}{n}\log\left(\frac{[reduced\ form]}{[oxidized\ form]}\right) \text{ ------ [3]}$$

Where $E_{applied}$ is the applied potential of working electrode, $E^{0'}$ is the formal potential of the reaction and n is the number electron in the redox reaction. For calculate of the percentage of reduced species as a function of potential Soret band and B band intensity as function of voltage is considerate.

Operando UV-vis spectroscopy:

Operando UV – vis spectroscopy is performed in a three electrode an optically transparent thin layer electrochemical cell (OTTLE) which schematic shown below. Working electrode (WE) (1×1 cm^2 Pt mesh) and counter electrode (CE) (Pt wire) is placed in 1 mm thickness path length of the cuvette and the reference electrode (Ag/AgCl) is placed in top of the working electrode (10 mm pathlength). For the gas inlet and gas outlet hole is present to purge the electrolyte before the experiment and maintain the inert atmosphere during experiment. All the data is collected in AutoLab UB spectrophotometer (Metrohm) in DIO trigger mode with deuterium /halogen light source. The data is collected in 200 to 800 nm wavelength with integration time of 25 ms with 100 number of spectra averages. During the data collection sampled DC voltammogram is performed with a 5mV voltage pulse for 30 sec. Before the experiment, electrolyte is purged for 30 min with the flow rate of 150 mL/min in the air sealed cell and keep the gas flow top of the solution to maintain the inert atmosphere (anaerobic condition). The beam is incident on the working electrode surface to monitor electronic energy state changes during the redox process which is shown in schematic.

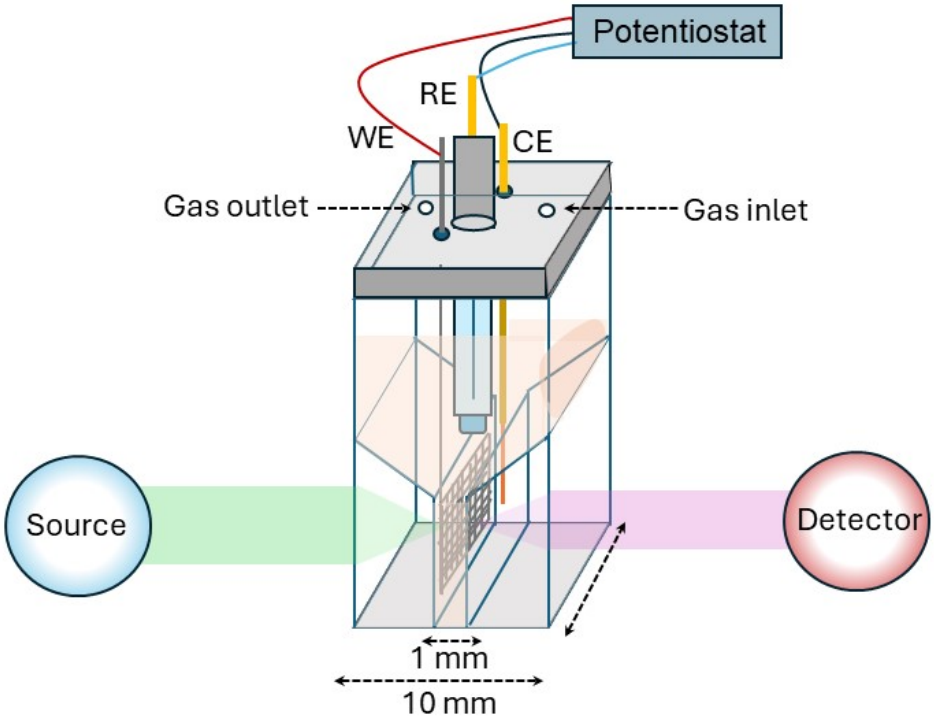

Schematic 1: Operando UV-vis spectroscopy experimental set up. The pathlength of the light is 1 mm where WE and CE electrode is placed and reference electrode top of them. All three electrode is connected to a potentiostat for apply the voltage pulse. The light beam is focused on the working electrode surface.

Operando circular dichroism:

Operando circular dichroism experiment is carried out an inhouse build electrochemical set up which schematic is shown below. The experiment is done in nitrogen atmosphere. The electrolyte is purged at the flow rate of 150 mL/min for 30 min and maintain the gas flow during data collection. The data is collected for 60 sec of accumulation time with averaging 2 times of the spectrum. During data collection, sampled DC voltammogram is performed with a 50 mV voltage pulse for 120 sec in each step. The working and reference electrode is connected with potentiostat (AutoLab, Metrohm).

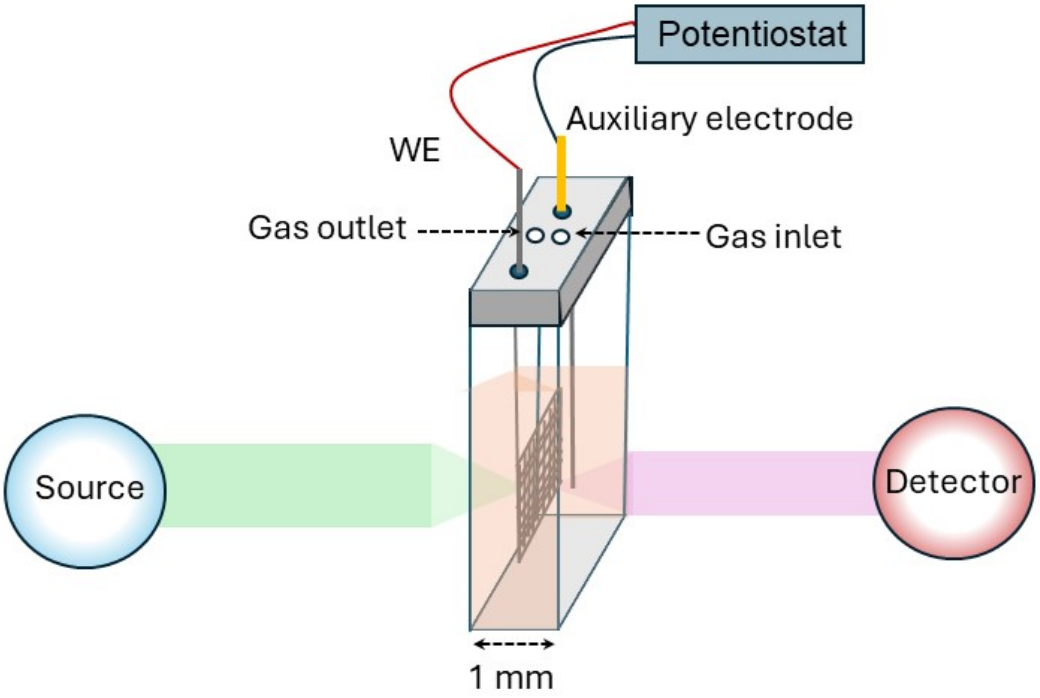

Schematic 2: Operando circular dichroism experimental set up. The pathlength of the cuvette is 1 mm. Gas inlet and outlet is there to purge the electrolyte and maintain the inert atmosphere.

Operando Raman experiment:

Operando Raman experiments are carried out in house build operando electrochemical cell which schematic is given bellow. In this cell, quartz window is used for the Raman transparent window. The distance of the window and working electrode is 2 mm to minimize the interference of the lessor beam by the window as well as electrolyte. The volume of the electrolyte is used 1.5 mL in this cell. In the below and upper part of the cell is tight with screw with an O ring to air tight the cell. Reference and counter electrode are inserted inside cell with the side wall of the cell. To minimize the distance of the distance of the CE, RE and WE, all three electrode is precisely placed in small volume of the electrolyte. All the experiment is done in inert atmosphere where the electrolyte (PBS buffer) is purged before the experiment at 150 mL/min of flow rate for 30 min. Horiba confocal Raman instrument is used for the experiment where 50 XL lense is use for focusing and 633 nm lessor source is used for the experiment with 25 % of power with 500

(600 nm) grading (schematic3). The resolution of spectrometer is 1 cm^{-1}. The spot size of the laser is used 2×2 μm^2.

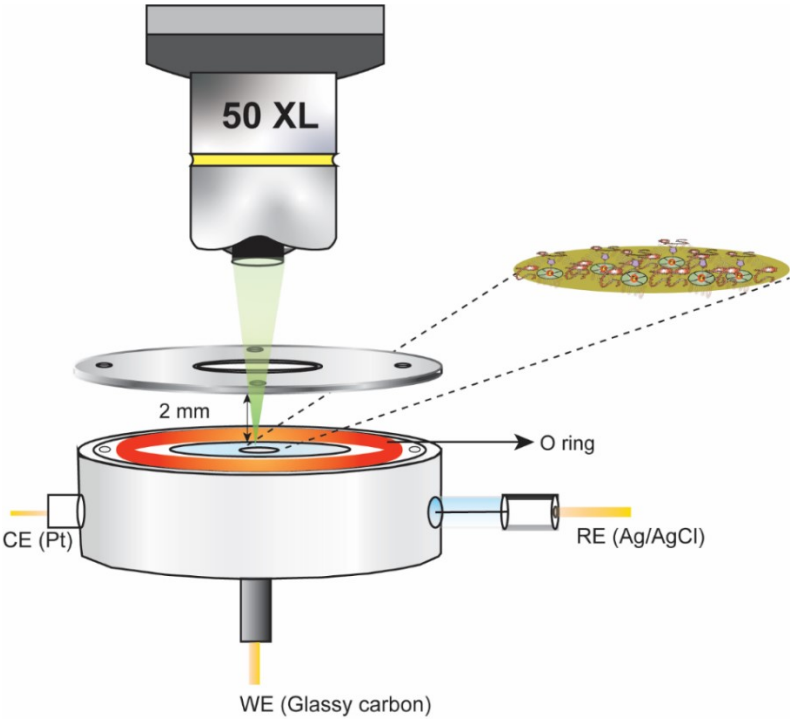

Schematic 3: Electrochemical cell for operando Raman spectroscopy measurements. The working electrode is covered with the thin film of protein molecules.

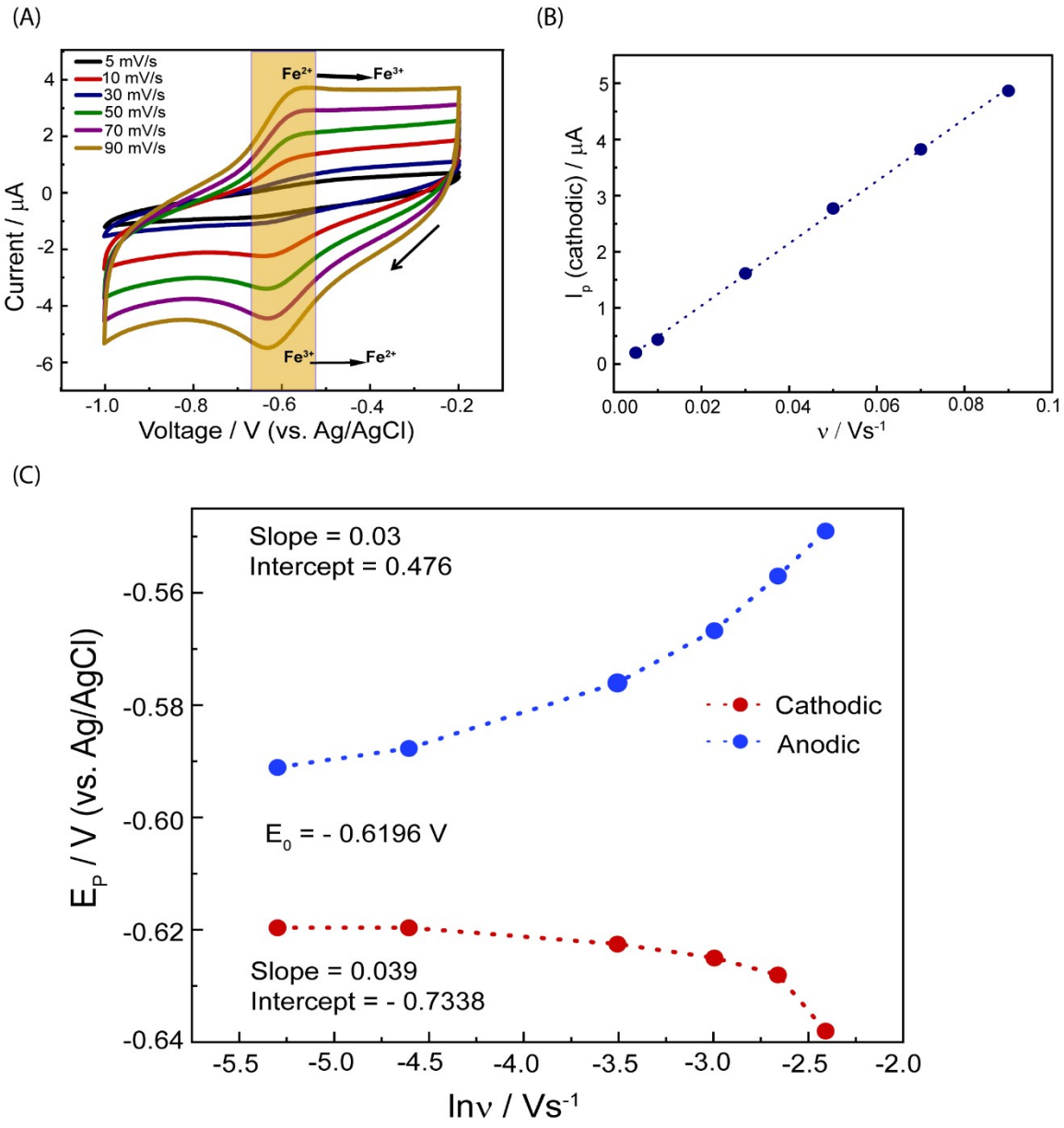

Figure S1. (A) Cyclic Voltammogram of hemin in PBS buffer at different scan rates. The arrow represents the scan direction. (B) Cathodic peak current versus ν plot indicates a linear relationship due to the surface adsorbed electron transfer process. (C) Plot of peak position (cathodic and anodic) versus lnν used in the estimation of rate constant and transfer coefficient as per the Laviron model.

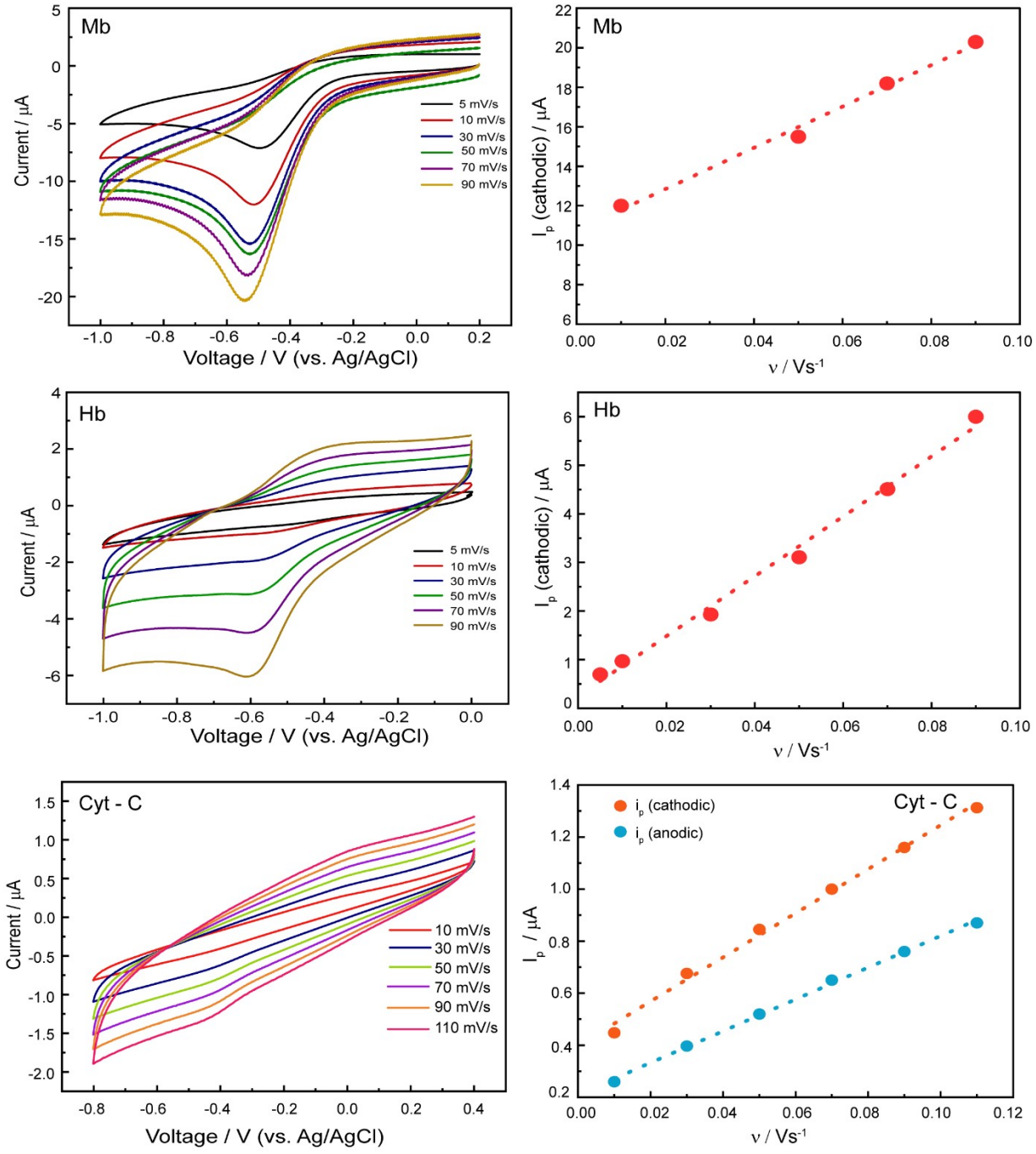

Figure S2. Cyclic Voltammogram of myoglobin (Mb) and hemoglobin (Hb) in left pannel in PBS (pH 7.2) buffer. Scan rate versus cathodic peak current for validation of surface adsorption process in the right panel.

Table S1. Heterogeneous rate constant and transfer coefficient of heme proteins as obtained from Laviron equation.[1]

	α_{System} / α_{Hemin}	K_{System} / K_{Hemin}
Myoglobin	0.693	0.423
Hemoglobin	0.66	0.245
Cytochrome C	0.25	0.89

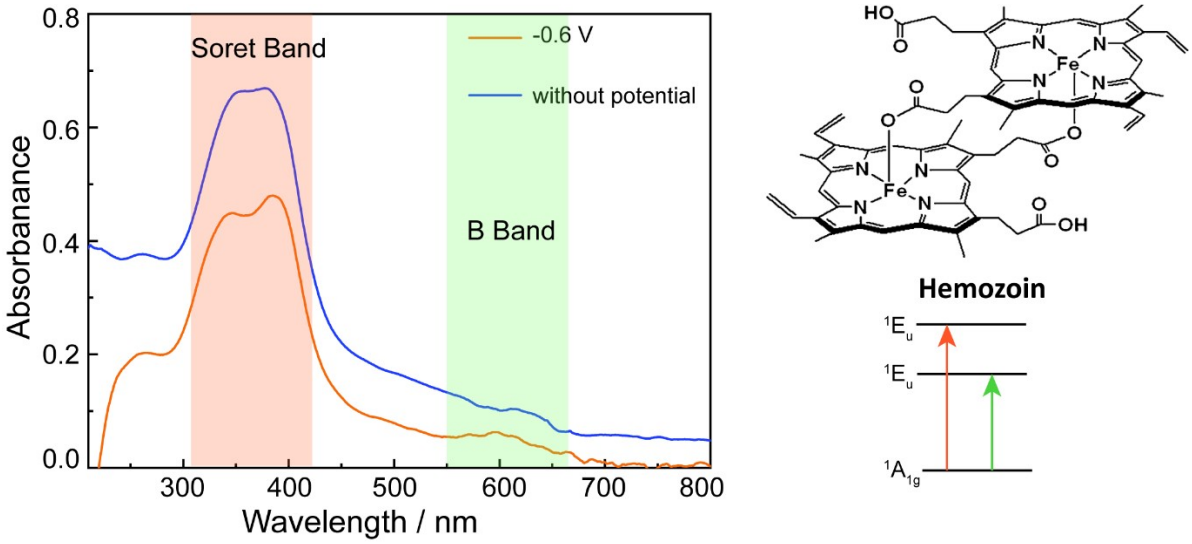

Figure S3. UV-vis spectra of hemin before and after application of potential. Under the application of potential, the hemozoin formation is shown in right side where the carboxylate group of the porphyrin ring coordinate to the iron center. The Soret band is due to the transition of electron from $^1A_{1g}$ to ^1E_g state and B band due to $^1A_{1g}$ to ^1E_u.

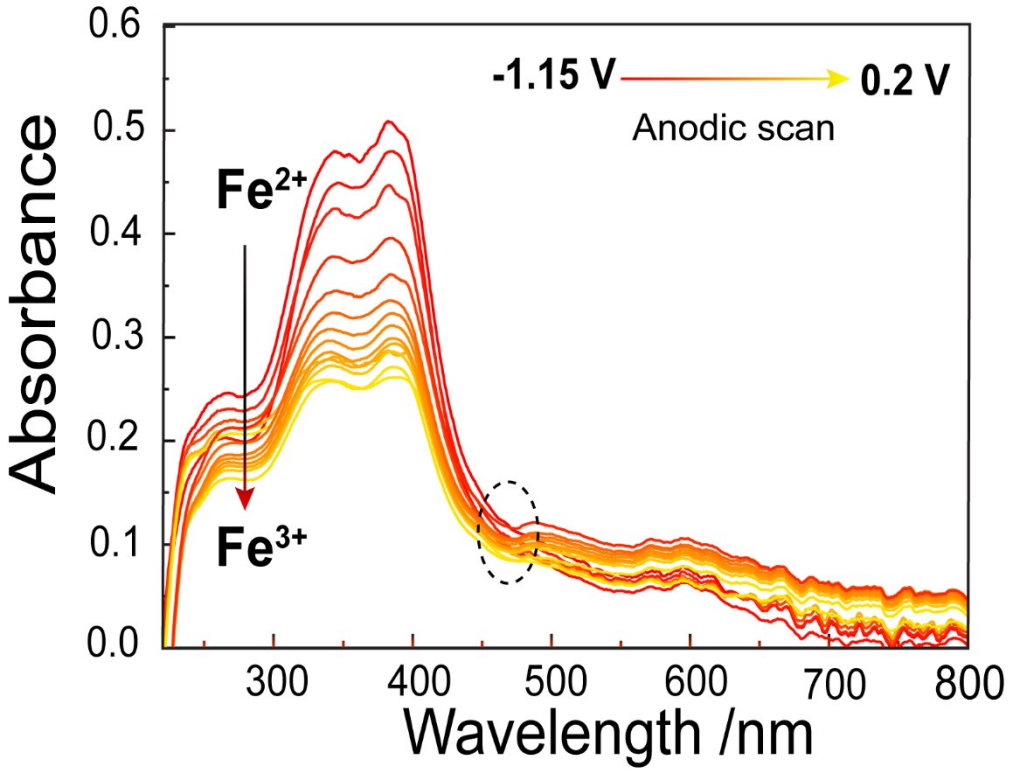

Figure S4. *Operando* UV-vis spectra of hemin in PBS buffer during oxidation of $Fe^{2+} \rightarrow Fe^{3+}$.

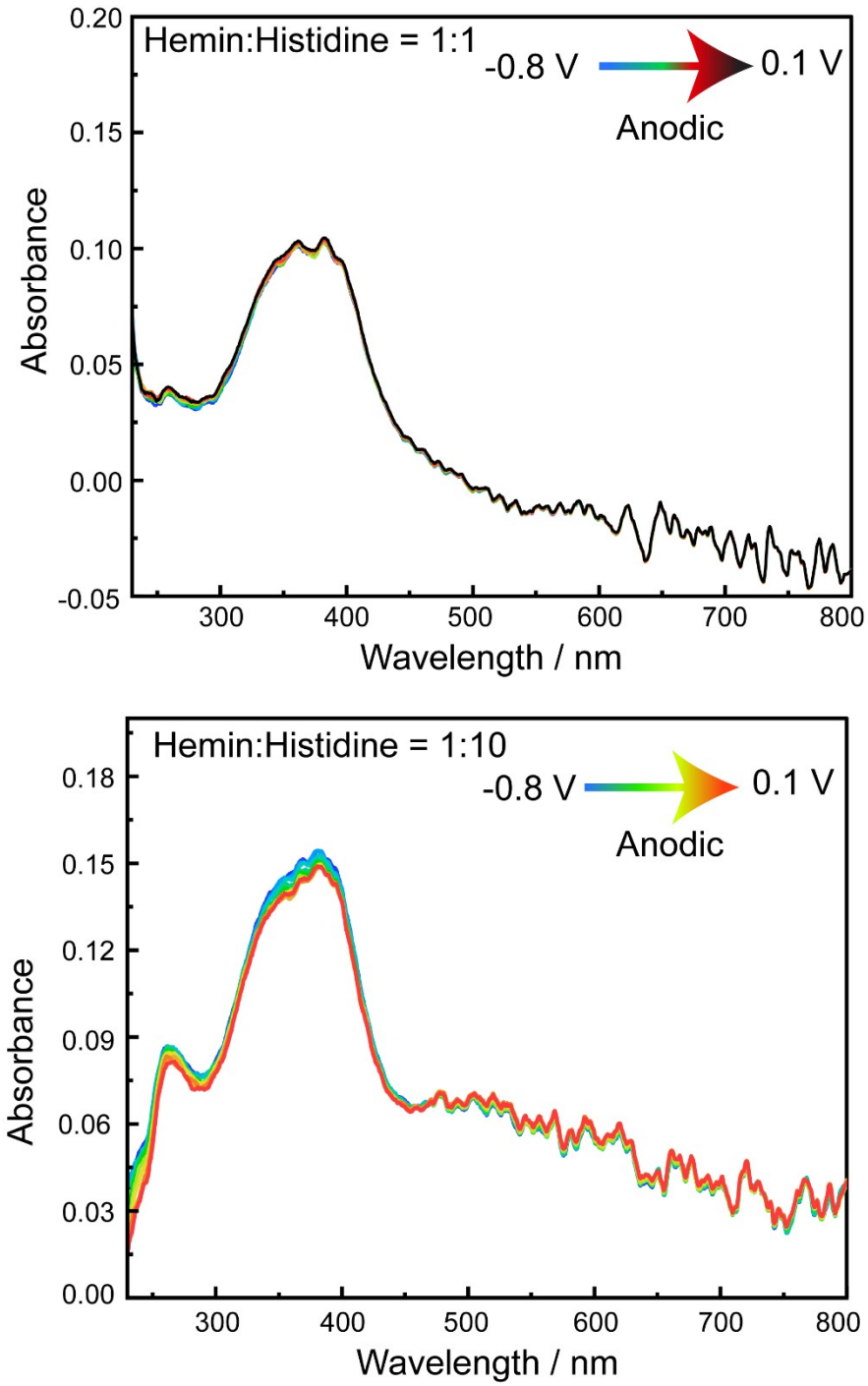

Figure S5. *Operando* UV-vis Spectra of Hemin and histidine mixture during the oxidation. The top one is for 1:1 and the bottom one is for 1:10 mixture.

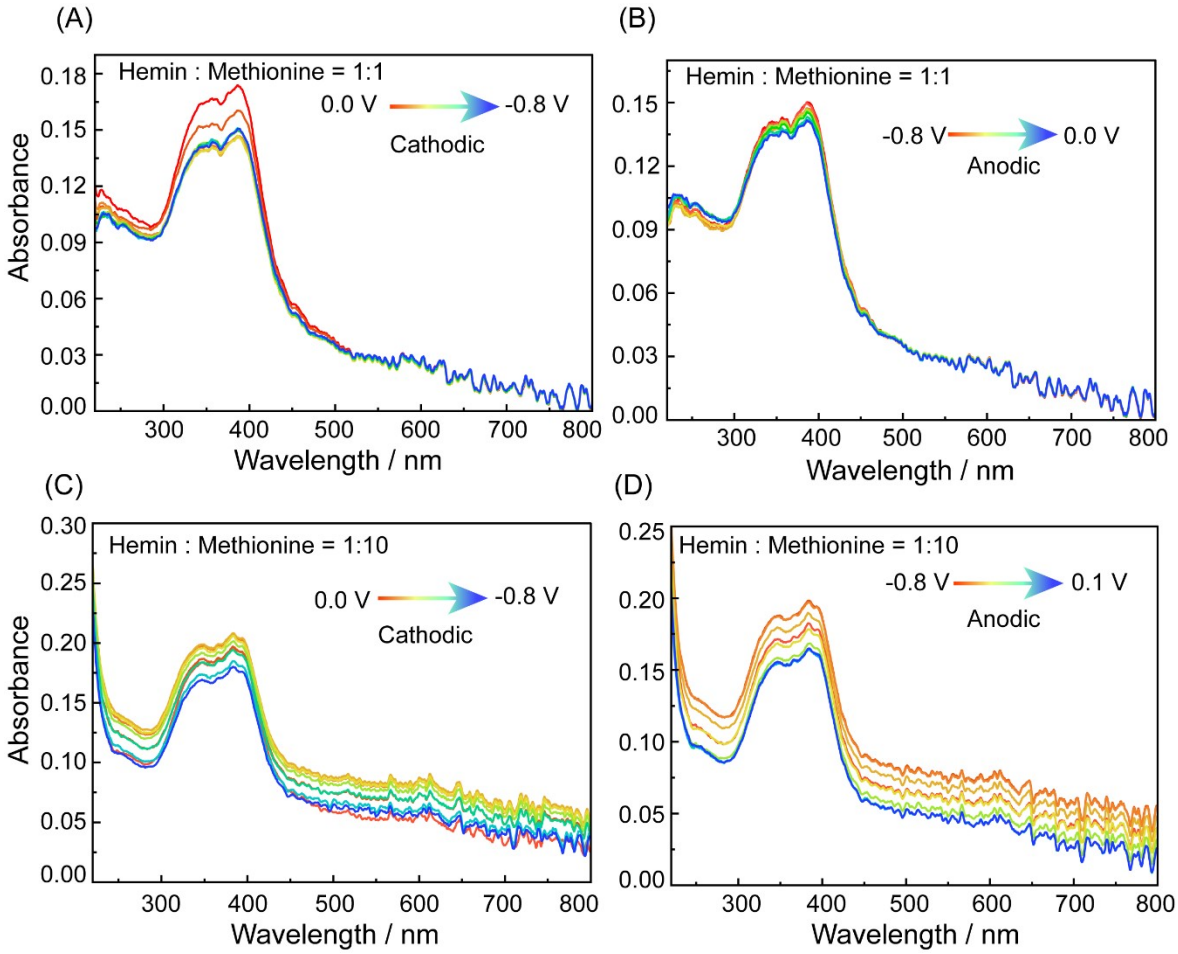

Figure S6. *Operando* UV-vis spectroscopy of hemin and methionine mixture. (A) and (B) 1:1 mixture of hemin and methionine during reduction and oxidation process respectively. (C) and (D) are for the 1:10 ratio of hemin : methionine mixture during the cathodic and anodic processes respectively.

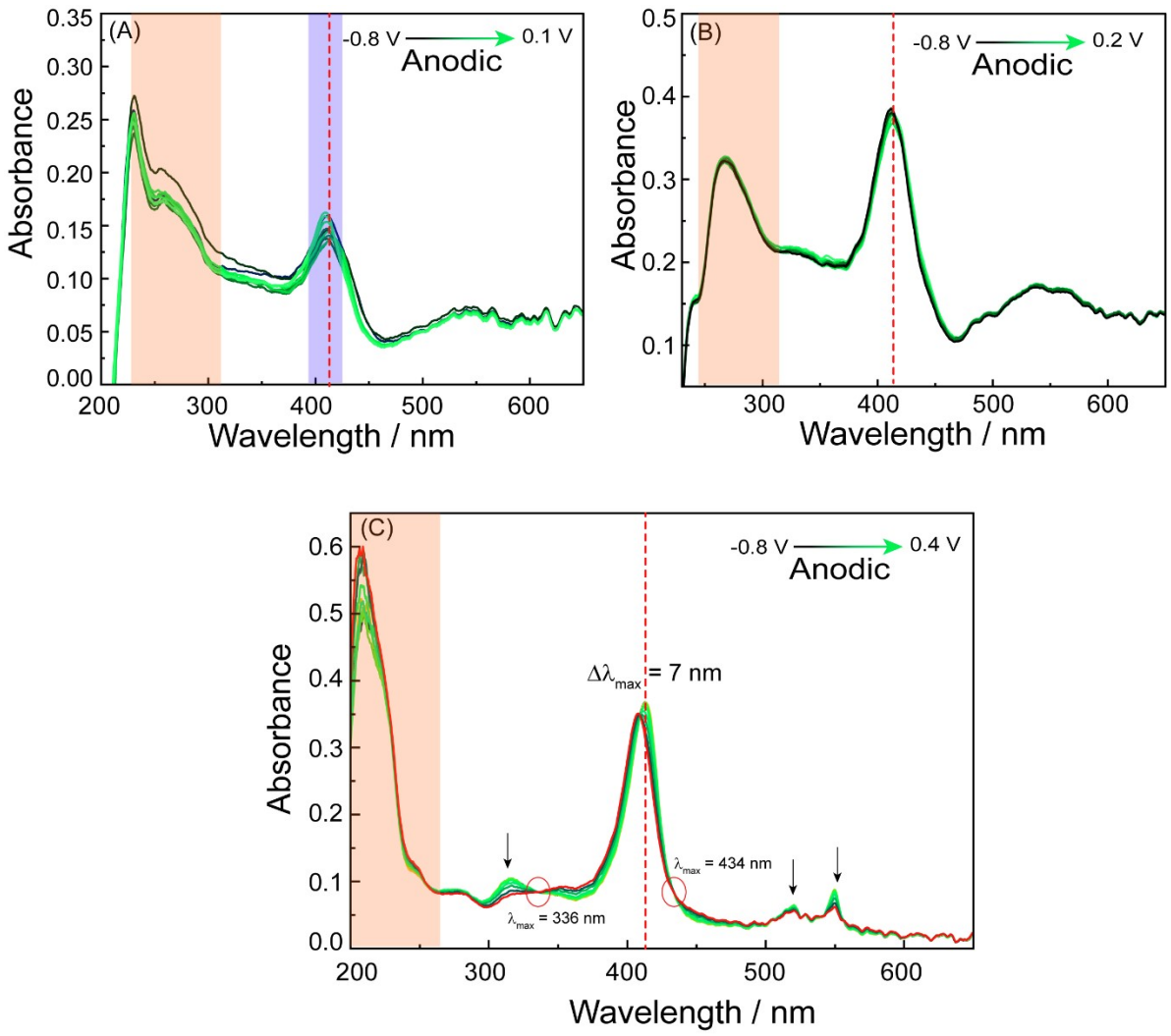

Figure S7. *Operando* UV-vis spectra during anodic process for (A) myoglobin (Mb), (B) hemoglobin and (C) cytochrome – C.

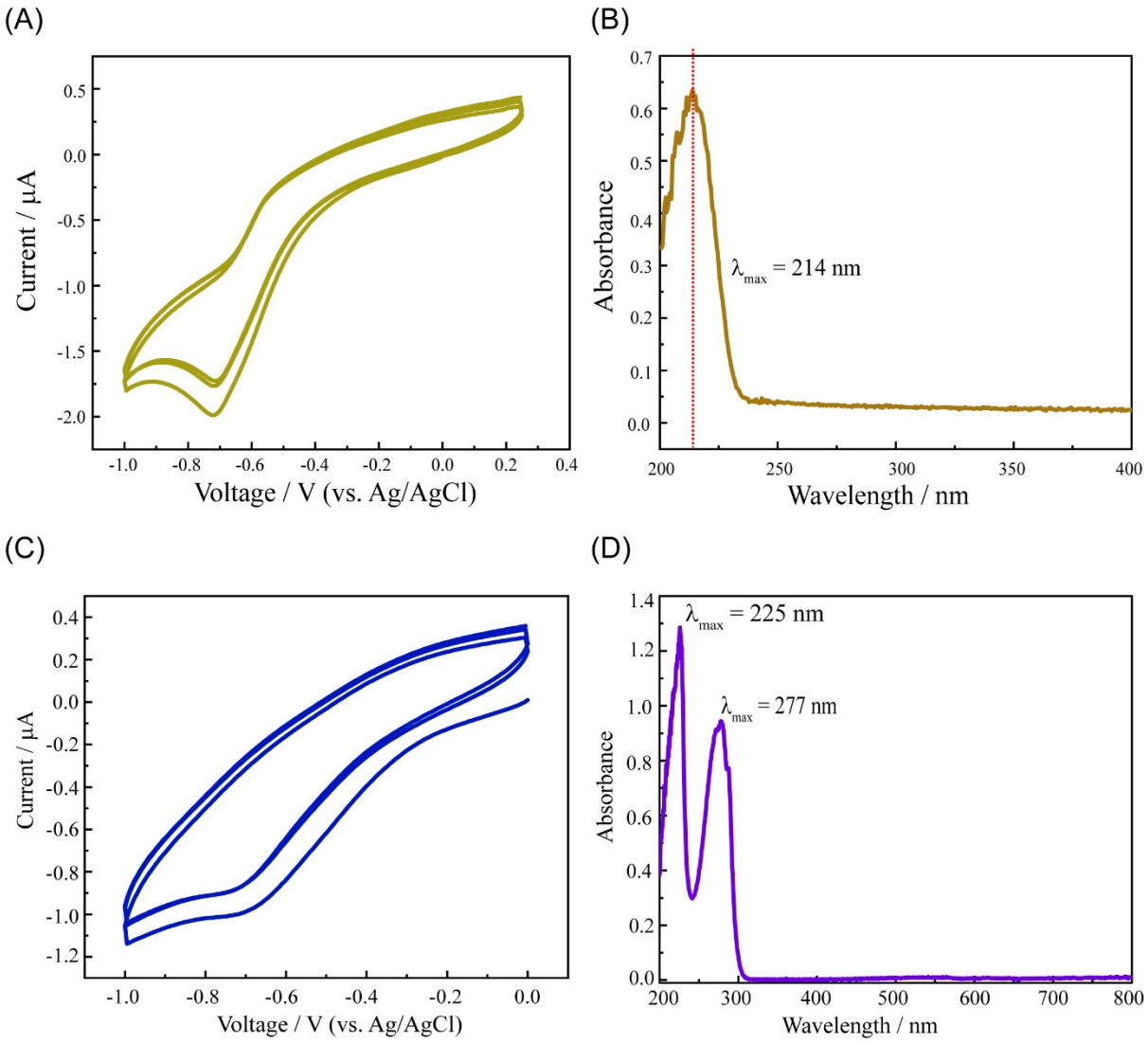

Figure S8. Cyclic voltammogram in PBS buffer for histidine (A) and tryptophan (C). UV -vis spectra in PBS buffer for histidine (B) and tryptophan (D) before application of voltage. The redox peak between -0.6V to -0.8V is due to the direct electrochemical deprotonation of the terminal primary amine (NH^{3+}) of histidine and tryptophan. The absorbance band near 214 nm due to the $\pi - \pi^*$ transition.[2,3]

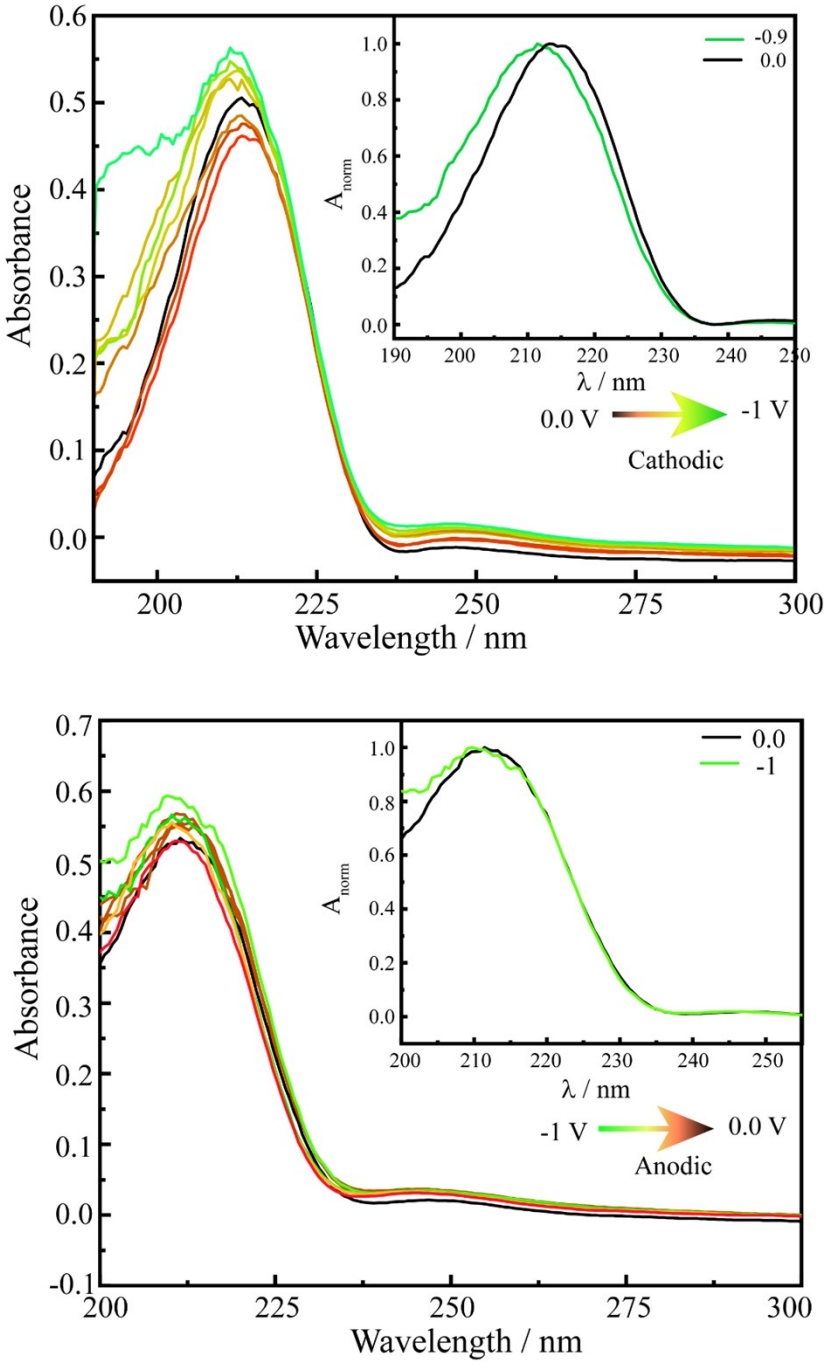

Figure S9. *Operando* UV-vis spectroscopy of histidine during reduction (top) and oxidation (below) graph. The π – π* transition during the redox process is shifted during the redox process due to direct electrochemical deprotonation of the amino acid leads to change in the energy state.

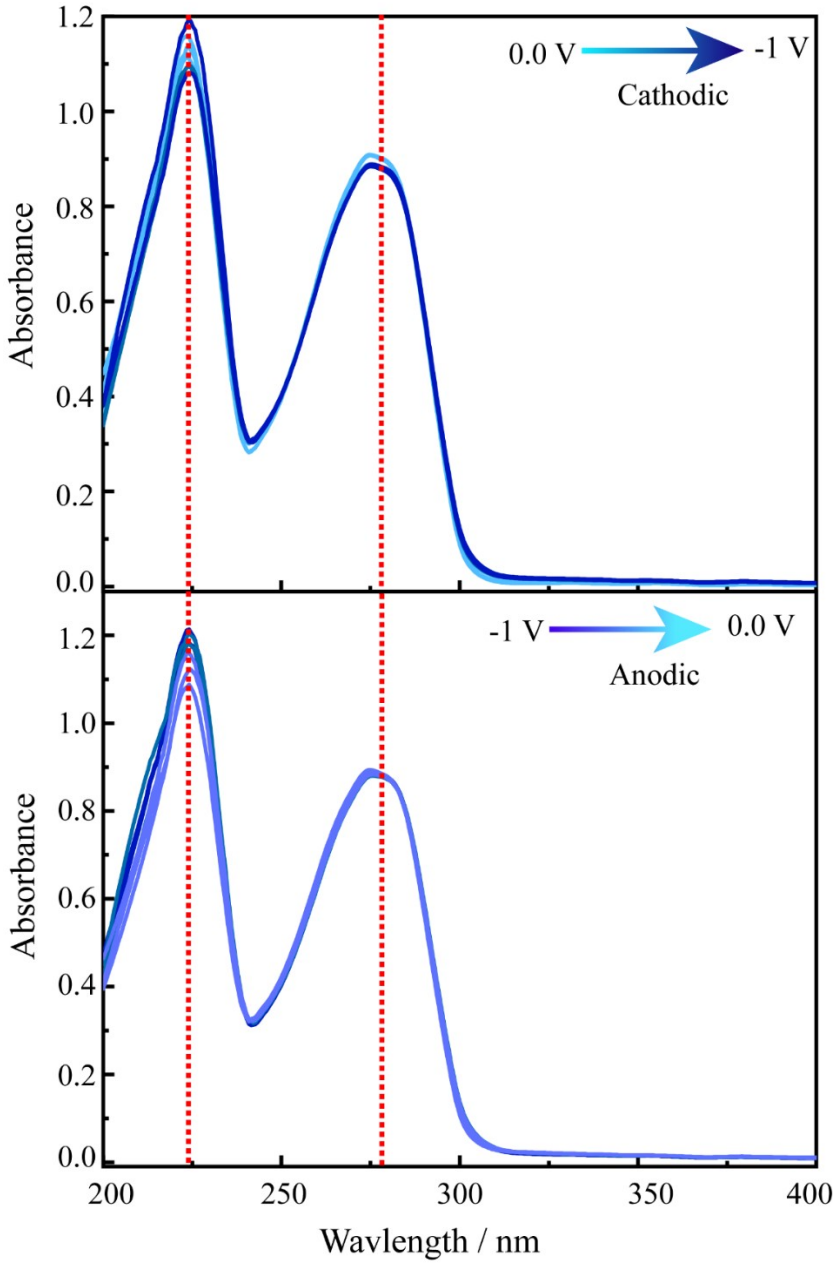

Figure S10. *Operando* spectroscopy of tryptophan during reduction (top) and oxidation (bottom). During individual redox chemistry of amino acid, the electrochemical deprotonation of the side chain amino acid used to happen. Thus, the effect on UV-vis spectra during the redox process is negligible on the aromatic ring.

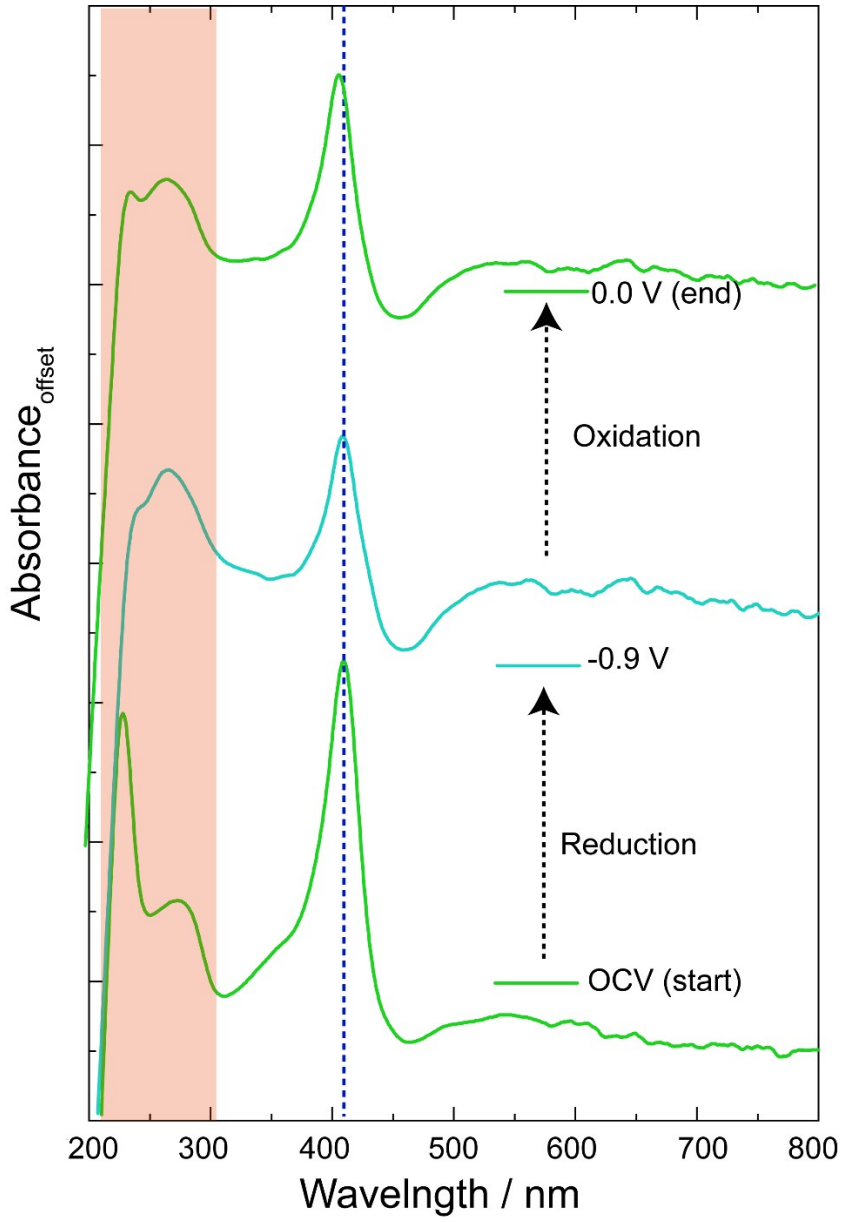

Figure S11. UV-vis spectra of myoglobin (Mb) in PBS buffer (pH 7.2) without any electrical field (at OCV) and after the first reduction cycle (-0.9 V) and after the first oxidation cycle (0.0 V). The absorbance band at 282 nm and 227 nm band merge together when the reduction occurs at the metal center which is shown in light red color. During cathodic process, the band separates slightly, however, the profile of the bands are significantly different from that at OCV.

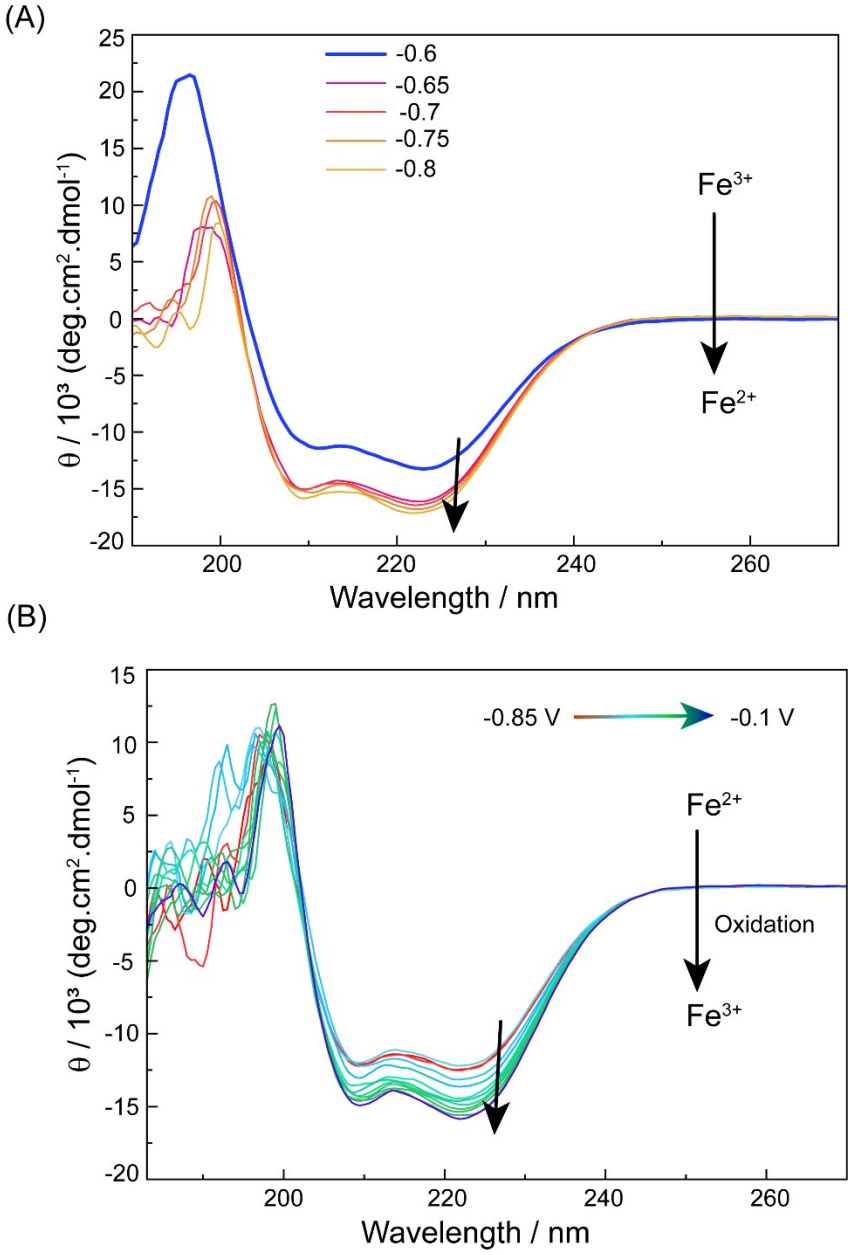

Figure S12. *Operando* circular dichroism after the maximum of the cathodic peak potential region for hemoglobin (A) and during the oxidation process (B) The α helicity peak of negative absorbance increases during the reverse process (**Fig. S12 (B)**). But the helicity is not reached the initial state may be due to the irreversible redox process.

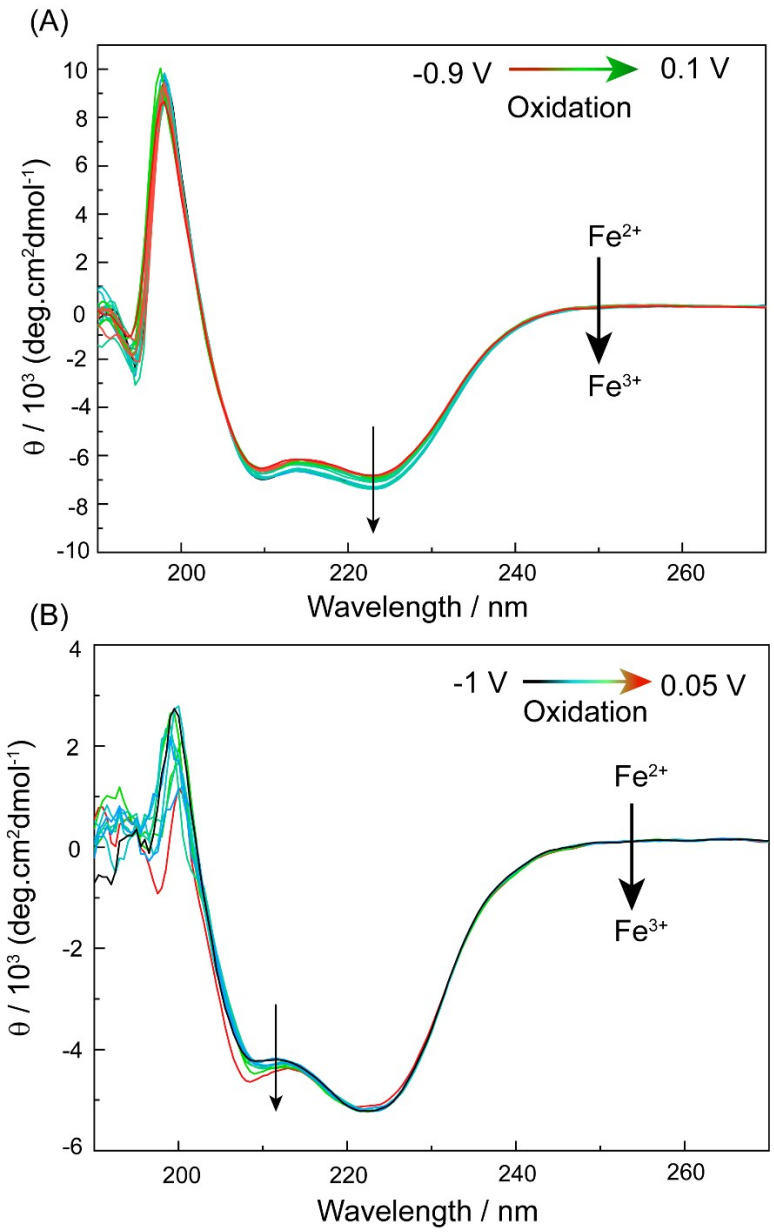

Figure S13. *Operando* circular dichroism during oxidation (A) myoglobin and (B) cytochrome - C.

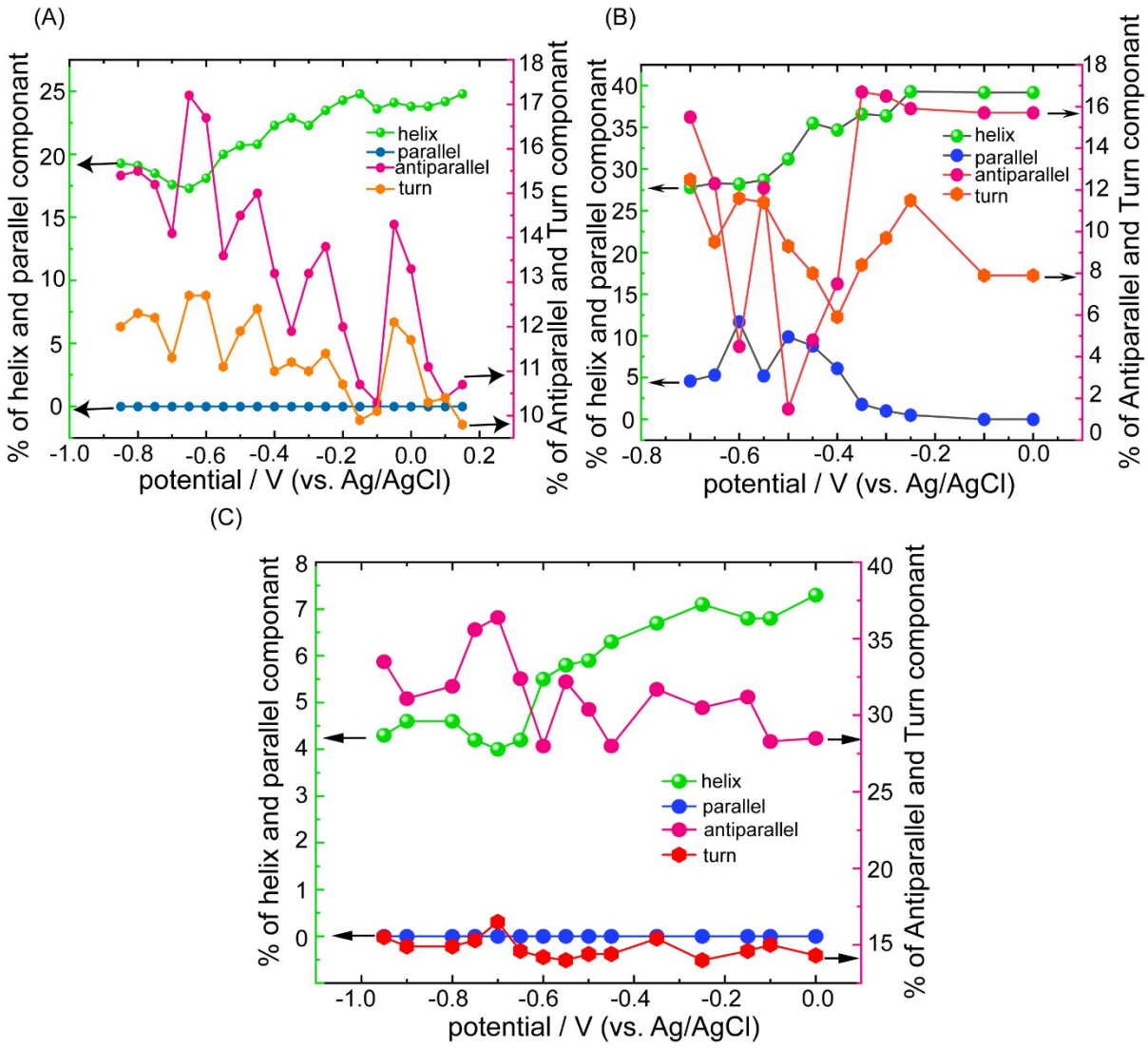

Figure S14. Change of secondary structural components during the reduction process for (A) myoglobin, (B) hemoglobin and (C) cytochrome – C.

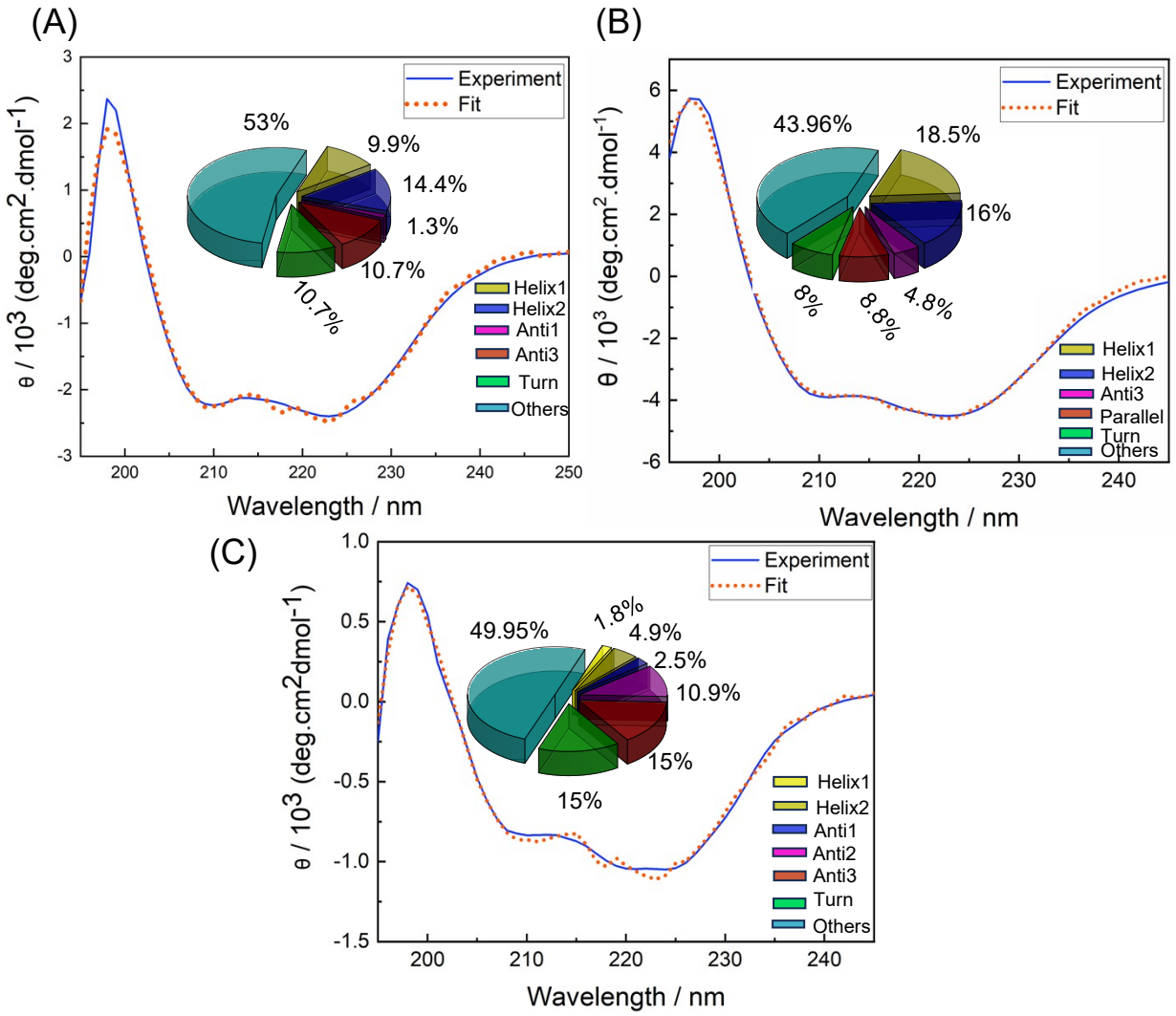

Figure S15. Pie chart diagram and BeStSel fitting data of Mb and the secondary structural component of (A) myoglobin, (B) hemoglobin and (C) cytochrome – C.

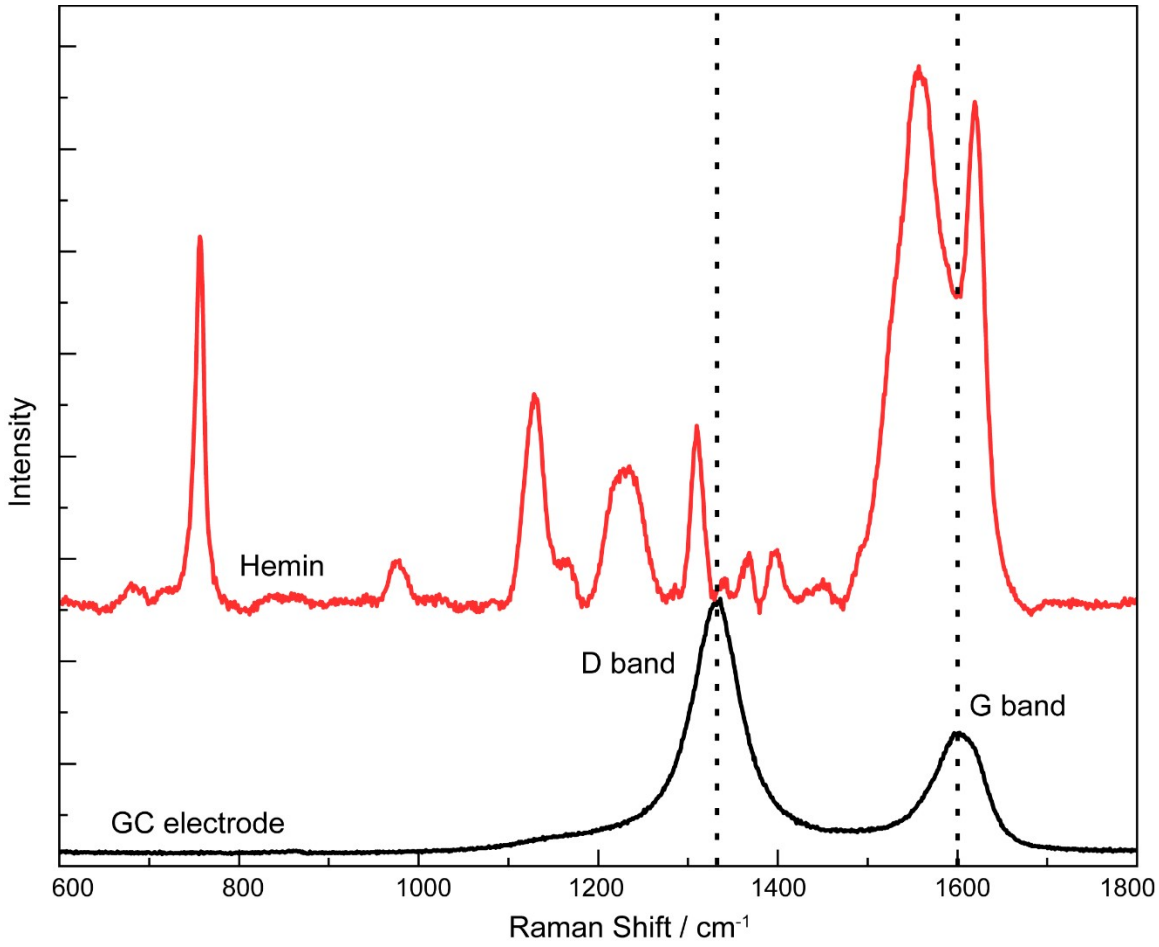

Figure S16: Raman spectra of Glassy carbon electrode and hemin cast on glassy carbon electrode inside the electrochemical cell in presence of electrolyte. As the glassy carbon electrode is covered by the thin film of the hemin, the D and G band is not observed for the modified electrode.

Table S2: Structural components of Hemoglobin during reduction from BeStSel fitting.

Potential(V)	*Helix*	*Helix1 (Regular)*	*Helix1 (distorted)*	*Antiparallel*	*Anti1 (Left twisted*	*Anti2 (relax)*	*Anti3 (Right twisted)*	*parallel*	*turn*	*others*
0	39.2	23.8	15.4	15.7	0	0	15.7	0	7.9	37.2
-0.1	39.2	23.8	15.4	15.7	0	0	15.7	0	7.9	37.2
-0.25	39.3	26.7	12.6	15.9	0	0	15.9	0.5	11.5	32.8

-0.3	36.4	24.2	12.2	16.5	0.2	0	16.3	1	9.7	36.4
-0.35	36.6	23.8	12.8	16.7	0.9	0	15.8	1.8	8.4	36.4
-0.4	34.7	18.4	16.3	7.5	0	0	7.5	6.1	5.9	45.9
-0.45	35.5	18.5	16	4.8	0	0	4.8	8.8	8	44
-0.5	31.2	17.4	13.8	1.5	0	0	1.5	9.9	9.3	47.9
-0.55	28.7	17.5	11.2	12.1	0	0	12.1	5.2	11.4	42.6
-0.6	28.2	15.5	12.7	4.5	4.5	0	0	11.7	11.6	44
-0.65	28.3	16.3	12.1	12.3	0	0	12.3	5.3	9.5	44.5
-0.7	27.8	18.4	9.4	15.5	0	0	15.5	4.6	12.5	39.6
-0.75	27.9	16.8	11.1	13.5	0	0	13.5	4.4	9.7	44.4
-0.8	27.8	18.4	9.4	15.5	0	0	15.5	4.6	12.5	39.6

Table S3: Structural components of myoglobin during reduction from BeStSel fitting.

Potential(V)	***Helix***	***Helix1 (Regular)***	***Helix1 (distorted)***	***Antiparallel***	***Anti1 (Left twisted***	***Anti2 (relax)***	***Anti3 (Right twisted)***	***parallel***	***turn***	***others***
0.15	24.8	9.8	15	10.7	0	0	10.7	0	9.8	54.7
0.1	24.2	9.8	14.3	10.4	1.7	0	8.7	0	10.4	55

0.05	23.8	9.8	14	11.1	2.2	0	9	0	10.3	54.8
0	23.8	10.1	13.7	13.3	3.2	0	10.1	0	11.7	51.2
-0.05	24.1	10.2	13.9	14.3	3.8	0	10.6	0	12.1	49.5
-0.1	23.6	9.3	14.2	10.3	1.2	0	9.1	0	10.1	56.1
-0.15	24.8	9.8	15	10.7	0	0	10.7	0	9.9	54.6
-0.2	24.3	9.9	14.4	12	1.3	0	10.7	0	10.7	53
-0.25	23.5	9.7	13.8	13.8	3.4	0	10.4	0	11.4	51.3
-0.3	22.3	8.5	13.8	13.2	2.5	0	10.7	0	11	53.5
-0.35	22.9	9.6	13.3	11.9	3.4	0	8.5	0	11.2	54
-0.4	22.3	8.5	13.8	13.2	2.5	0	10.7	0	11	53.5
-0.45	20.8	8.3	12.5	15	5.3	0	9.8	0	12.4	51.8
-0.5	20.7	7.9	12.7	14.5	4.7	0	9.8	0	11.9	52
-0.55	20	7.9	12.1	13.6	4.7	0	8.9	0	11.1	55.4
-0.6	18.1	6.7	11.4	16.7	6.6	0.1	9.9	0	12.7	52.5
-0.65	17.3	6.5	108	17.2	6.5	0.9	9.7	0	12.7	52.7
-0.7	17.6	7.1	11.8	14.1	4.9	0	9.2	0	11.3	55.8
-0.75	18.5	7.1	11.3	15.2	6.7	0	9	0	12.2	54.2
-0.8	19.1	7.4	11.7	15.5	6.2	0	9.2	0	12.3	53.1
-0.85	19.3	7	12.4	15.4	4.8	0	10.7	0	12	53.3

Table S4: Structural components of Cytochrome C during reduction from BeStSel fitting.

Potential(V)	*Helix*	*Helix1 (Regular)*	*Helix1 (distorted)*	*Antiparallel*	*Anti1 (Left twisted*	*Anti2 (relax)*	*Anti3 (Right twisted)*	*parallel*	*turn*	*others*
0	7.3	2.1	5.3	28.5	7	7.6	13.8	0	14.3	49.8
-0.1	6.8	1.8	4.9	28.3	2.5	10.9	15	0	15	50
-0.15	6.8	1.9	4.9	31.2	7.2	9.3	14.7	0	14.6	47.3
-0.25	7.1	2.2	5	30.5	9	8	13.6	0	14	48.4
-0.35	6.7	1.8	5	31.7	2.8	13.2	15.7	0	15.4	46.2
-0.45	6.3	1.5	4.9	28	9	5.1	14	0	14.4	51.2
-0.5	5.9	1.4	4.6	30.4	7.1	9.3	14	0	14.4	49.2
-0.55	5.8	1.4	4.4	32.2	8.8	9.6	13.8	0	14	47.9
-0.6	5.5	0.9	4.6	28	5.7	8.9	13.4	0	14.2	52.3
-0.65	4.2	0.4	4.2	32.4	8.5	9.5	14.4	0	14.6	48.4
-0.7	4	2.5	1.5	36.4	0	18.8	17.5	0	16.5	43.1
-0.75	4.2	0.5	3.7	35.6	4.3	15.7	15.5	0	15.3	45
-0.8	4.6	0.6	4	31.9	7.8	9.2	14.9	0	14.9	48.6
-0.9	4.6	0.8	3.9	31.1	6.4	9.7	15	0	14.9	49.4
-0.95	4.3	0.6	3.7	33.5	1.5	16.4	15.6	0	15.5	46.7

Table S5: Band assignments, symmetry terms and local coordination of hemin at the initial state. All the bands are well matched with the literature.[4-7] Some of the bands are small deviated probably due to electrolyte interference. The notation of the mode as follows: ν = in - plane stretching mode ϒ = out of plane mode and δ = deformation mode.

Band Position(cm^{-1})	***Assignment***	***Symmetry term***	***Local Coordination***
*1623**	ν_{10}	B_{1g}	$\nu(C_\alpha C_m)_{asym}$
*1556**		B_{1g}	$\nu(C_\beta C_\beta)$
*1488**		A_{1g}	$\nu(C_\alpha C_m)_{sym}$
*1446**		E_u	$\nu(C_\alpha C_m)_{sym}$
1398	ν_{29}	B_{2g}	ν(pyrrole quarter ring)
1366			ν(C-N)
1308		A_{2g}	$\delta(C_mH)$
*1234**		E_u	$\delta(C_mH)$
1167	ν_{30}	B_{2g}	ν(pyrrole half ring)$_{asym}$
1120		A_{2g}	$\nu(C_\alpha N)$
974	ν_{46}	E_u	$\delta(\text{pyrrole deform})_{asym}$
*819**		B_{1u}	$\Upsilon(C_mH)$
754	ν_{15}	B_{1g}	ϒ(pyrrole breathing)
*675**	ν_7	A_{1g}	$\delta(\text{pyrrole deform})_{sym}$
405			$\delta(C_\alpha C_\beta C_m)$

345	ν(Fe-N)

REFERENCES

1. E. Laviron, *J. Electroanal. Chem. Interfacial Electrochem.*1979, **101,** 19–28.
2. M.O. Iwunze, *Journal of Photochemistry and Photobiology A: Chemistry* 2007, **186,** 283–289.
3. B. Malfoy, J.A. Reynaud, *J. Electroanal. Chem.* 1980, **114,** 213-223.
4. T. G. Spiro, *Biochimica et Biophysica Acta,* 1975*,* **416,** 169-189.
5. B. R. Wood, D. Mcnaughton, *J. Raman Spectrosc* 2002, **33,** 517 – 523.
6. L. Rimai, I. Salmeen, D. H. Petering, *Biochemistry* 1975, **14,** 378 – 382.
7. B. R. Wood, S. J. Langford, B. M. Cooke, J. Lim, F. K. Glenister, M. Duriska, J. K. Unthank, D. McNaughton, *J. Am. Chem. Soc.* 2004, **126,** 9233 – 9239.